25. Kobayashi H, Asano R, Oka T, et al. Simultaneous evaluation of myocardial perfusion and fatty acid metabolism using dynamic SPECT with single injection of ^{123}I-15-(p-iodophenyl)-3-methyl pentadecanoic acid (BMIPP). *Jpn J Nucl Med* 1995;32:19–29.
26. Tamaki N, Tadamura E, Kawamoto M, et al. Decreased uptake of iodinated branched fatty acid analog indicates metabolic alterations in ischemic myocardium. *J Nucl Med* 1995;36:1974–1980.
27. Schwaiger M, Schelbert HR, Ellison D, et al. Sustained regional abnormalities in cardiac metabolism after transient ischemia in the chronic dog model. *J Am Coll Cardiol* 1985;6:336–346.
28. Nienaber CA, Brunken RC, Sherman CT, et al. Metabolic and functional recovery of ischemic human myocardium after coronary angioplasty. *J Am Coll Cardiol* 1991;18:966–978.
29. Matsuzaki M, Gallagher KP, Kemper WS, White F, Ross J Jr. Sustained regional dysfunction produced by prolonged coronary stenosis: gradual recovery after reperfusion. *Circulation* 1983;68:170–182.
30. Topol EJ, Weiss JL, Guzman PA, et al. Immediate improvement of dysfunctional myocardial segments after coronary revascularization: detection by intraoperative transesophageal echocardiography. *J Am Coll Cardiol* 1984;4:1123–1134.
31. Carlson EB, Cowley MJ, Wolfgang TC, Vetrovec GW. Acute changes in global and regional rest left ventricular function after successful coronary angioplasty: comparative results in stable and unstable angina. *J Am Coll Cardiol* 1989;13:1262–1269.
32. Cohen M, Charney R, Hershman R, Fuster V, Gorlin R. Reversal of chronic myocardial dysfunction after transluminal coronary angioplasty. *J Am Coll Cardiol* 1988;12:1193–1198.
33. Van Den Berg EK Jr, Popma JJ, Dehmer GJ, et al. Reversible segmental left ventricular dysfunction after coronary angioplasty. *Circulation* 1990;81:1210–1216.
34. Vanoverschelde JLJ, Wijns W, Depre C, et al. Mechanisms of chronic regional postischemic dysfunction in humans: new insights from the study of noninfarcted collateral-dependent myocardium. *Circulation* 1993;87:1513–1523.
35. Tillisch J, Brunken R, Marshall R, et al. Reversibility of cardiac wall-motion abnormalities predicted by positron tomography. *N Engl J Med* 1986;314:884–888.
36. Tamaki N, Kawamoto M, Yonekura Y, et al. Assessment of fatty acid metabolism using ^{123}I branched fatty acid: comparison with positron emission tomography. *Ann Nucl Med* 1993;7(suppl II):SII-41–SII-47.
37. Franken PR, Dendale P, De Geeter F, Demoor D, Bossuyt A, Block P. Prediction of functional outcome after myocardial infarction using BMIPP and sestamibi scintigraphy. *J Nucl Med* 1996;37:718–722.
38. Hashimoto A, Nakata T, Tsuchihashi K, Tanaka S, Fujimori K, Iimura O. Postischemic functional recovery and BMIPP uptake after primary percutaneous transluminal coronary angioplasty in acute myocardial infarction. *Am J Cardiol* 1996;77:25–30.
39. Rocco TP, Dilsizian V, McKusick KA, Fischman AJ, Boucher CA, Strauss HW. Comparison of thallium redistribution with rest "reinjection" imaging for the detection of viable myocardium. *Am J Cardiol* 1990;66:158–163.
40. Dilsizian V, Rocco TP, Freedman NMT, Leon MB, Bonow RO. Enhanced detection of ischemic but viable myocardium by the reinjection of thallium after stress-redistribution imaging. *N Engl J Med* 1990;323:141–146.
41. Tamaki N, Tadamura E, Kudoh T, et al. Prognostic value of iodine-123 BMIPP fatty acid analogue imaging in patients with myocardial infarction. *Eur J Nucl Med* 1996;23:272–279.

Technetium-99m-MIBI Myocardial SPECT: Supine Versus Right Lateral Imaging and Comparison with Coronary Arteriography

Sherif I. Heiba, Nasser J. Hayat, Hani S. Salman, Ezzat Higazy, Mohammed E. Sayed, Zuhair Saleh, Ali I. Khalaf, Mohammed Naeem and Suhair Bourosly

Departments of Nuclear Medicine and Cardiology, Faculty of Medicine, Kuwait University, and Chest Hospital, Kuwait City, Kuwait

Myocardial perfusion SPECT using the prone position improves inferior wall counts and decreases motion problems as compared with the usual supine position. Nonetheless, it is not suitable for women. In addition, it is associated with artifactual anteroseptal defects and hot spots. **Methods:** The right lateral (RL) position was evaluated instead of the prone position in 72 patients (26 women). RL imaging was performed immediately after the supine imaging during a routine 2-day ^{99m}Tc-sestamibi exercise protocol. The SPECT images were scored semiquantitatively by three physicians. Moreover, regional myocardial counts, as well as extent and severity of defects, were assessed by quantitative polar map analysis. **Results:** All patients tolerated the RL position well and there was no significant patient movement in either position. Higher inferior myocardial counts per pixel were observed in the RL than in supine images. Inferior wall defects (especially mild ones) were more common in the supine than the RL images, whereas defects in other regions were not different. Quantitative analysis confirmed these findings. Analysis of 34 patients with recent coronary arteriography revealed an overall coronary artery disease (CAD) supine- and RL-imaging specificity of 50% and 75%, respectively, and the sensitivities of both were 93%. Right CAD sensitivity, specificity and normalcy rates for the supine position were 100%, 44% and 55%, whereas those of the RL position were 94%, 75% and 90%, respectively. **Conclusion:** The RL position improves CAD diagnostic accuracy, particularly right CAD, without significant artifacts in other myocardial regions. Unlike the prone position, the RL position is well tolerated by both women and men.

Key Words: technetium-99m-sestamibi; SPECT; myocardial perfusion; right lateral

J Nucl Med 1997; 38:1510–1514

Received May 17, 1996; revision accepted Dec. 10, 1996.

For correspondence or reprints contact: Sherif I. Heiba, MD, Department of Nuclear Medicine, Faculty of Medicine, Kuwait University, P.O. Box 24923, Safat, Kuwait 13110.

SPECT perfusion myocardial imaging is an accurate technique not only for the diagnosis of coronary artery disease (CAD) but also for the evaluation of the site and extent of jeopardized myocardium (*1–3*). Inferior wall attenuation by the left hemidiaphragm is a considerable problem that seriously contributes to imaging artifacts and the potential decrease of diagnostic accuracy (*4–10*). Image acquisition with patients in the prone position was promoted by some investigators to improve inferior wall counts (*11–14*), in addition to reducing motion problems when patients are unable to tolerate the supine position (*15*). The drawbacks of this method are contrasting septal artifacts as well as photon attenuation by the imaging table, unless a specially designed table is used. Furthermore, this technique is not suitable for women. Another method using the semidecubital position also requires a specially constructed imaging table and has yet to be proven (*16,17*).

The increased interest in attenuation correction and gated SPECT techniques to routinely eliminate attenuation artifacts reflects the importance of this common problem. Nonetheless, these new sophisticated methods are technically demanding and not widely accessible. A simple solution requiring no costly modifications or sophisticated new equipment is not yet available.

This study evaluated the ability of right lateral (RL) SPECT imaging to resolve inferior wall-count attenuation, explored whether this method could create any new artifacts and assess whether CAD diagnostic accuracy improves with this technique.

MATERIALS AND METHODS

Patient Population

We evaluated 72 patients (46 men, 26 women; mean age 50.0 ± 11.5 yr) who were scheduled for routine exercise ^{99m}Tc-sestamibi myocardial perfusion studies. Twenty patients had a low likelihood

TABLE 1
Patient Characteristics

Variables	Men (n = 46)	Women (n = 26)	p
Age	48.7 ± 12.2	52.6 ± 9.5	ns
Previous MI	21 (46%)	1 (4%)	<0.005
ECG Q wave	16 (35%)	1 (4%)	<0.005
Diabetes mellitus	11 (24%)	11 (42%)	<0.05
Hypertension	16 (35%)	12 (46%)	ns
CAD family history	10 (29%)	2 (13%)	ns
Smoking	27 (59%)	1 (4%)	<0.0001
Hyperlipidemia	5 (11%)	2 (8%)	ns
Sestamibi results			
Abnormal	35 (76%)	11 (42%)	<0.005
Fixed defect only	17 (37%)	2 (8%)	<0.01
Reversible defect	18 (39%)	9 (35%)	ns

CAD = coronary artery disease; MI = myocardial infarction; ECG = electrocardiogram; ns = not significant.

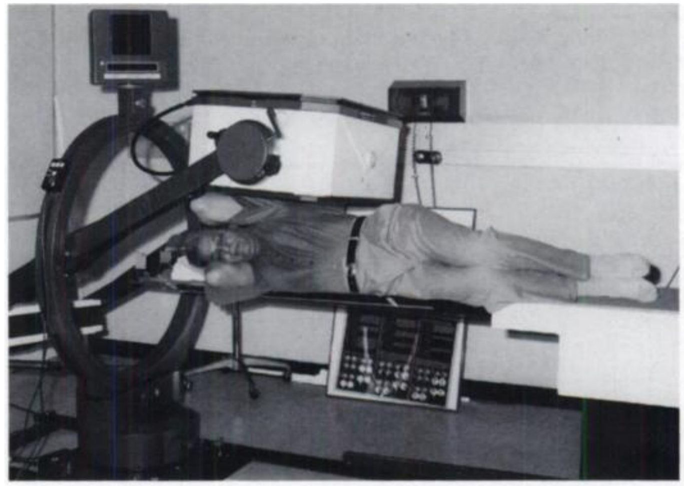

FIGURE 1. Demonstration of patient position on the imaging table using the RL SPECT technique.

of CAD. A history of previous myocardial infarction was documented in 22 patients; of those, 17 had Q-wave infarctions. Of 45 patient with coronary arteriography, 34 had recent (<3 mo) coronary arteriography and no interval myocardial infarction, revascularization procedure or deterioration of usual angina pattern. CAD by coronary arteriography was defined as lesions ≥50%. Thirteen patients had three-vessel disease, 11 had two-vessel disease, 7 had single-vessel disease, 3 had normal coronary arteries. Table 1 summarizes all patient characteristics.

Exercise Perfusion Imaging

Patients exercised on the treadmill using the Bruce protocol, reaching a peak exercise heart rate of at least 85% of their maximum predicted heart rate response before being injected with 740-1110 MBq (20–30 mCi) ^{99m}Tc-sestamibi. Initial supine SPECT images were obtained 1–2 hr later. Rest images were performed on another day using similar radioisotope doses. RL SPECT images were immediately obtained after the supine images. Patients were placed on the imaging table on their right side with their arms extended and both their hips and knees slightly flexed (Fig. 1). Thirty-two projection images were acquired in a 64 × 64 matrix over a 180° arc from 45° left posterior oblique to 45° right anterior oblique using step-and-shoot acquisition for 30 sec each in both supine and RL images. The SPECT studies were performed using a gamma camera equipped with a low-energy high-resolution collimator and interfaced with a dedicated computer. Filtered backprojected data were reconstructed into the usual three-axis slices.

Regional Myocardial Counts Assessment

Data from 20 patients with a low likelihood of CAD were used to compare myocardial counts in the supine and RL imaging positions. Myocardial polar maps were divided into five myocardial regions and applied equally to all patient data. Maximum and mean counts per pixel in each region were measured and summarized in male and female populations, both in the supine and RL SPECT images.

Quantitative and Semiquantitative Assessment

Comparable stress and rest slices of each patient were simultaneously displayed in the short axis and the vertical long axis. Images were divided into 20 segments and independently scored by three experienced observers using a 4-point scoring system (0 = normal, 1 = mildly reduced, 2 = moderately reduced and 3 = severely reduced or absent uptake). The defect was considered reversible when there was at least a 2-point uptake improvement in the rest images.

A commercially available polar map was used on all images to determine quantitatively the extent (number of pixels) and severity (number of s.d. below the pixel mean) of defects (*18*).

Evaluation of Patient Motion During Imaging

The frequency and severity of motion during data acquisition were reviewed and compared in each patient for the two imaging techniques. The raw data from each patient were examined in the cine mode and patient motion was scored using another 4-point scale (0 = no motion, 1 = slight motion, 2 = moderate motion and 3 = severe motion).

Statistical Analysis

Statistical analyses of various comparison factors were tested by χ^2 contingency table. Student's t-test was used in continuous variables. A p value < 0.05 was considered significant. Values are shown as the means ± 1 s.d. Sensitivity and specificity were used only on patients with recent coronary arteriography. A normalcy

TABLE 2
Comparison of Regional Myocardial Count Distribution with Respect to Apex between Supine and RL Imaging

	Men (n = 9)			Women (n = 11)			Total (n = 20)		
Region	Supine	RL	p	Supine	RL	p	Supine	RL	p
Apex	100	100	ns	100	100	ns	100	100	ns
Anterior	83.7 ± 5.4	83.8 ± 4.7	ns	79.6 ± 6.7	80.3 ± 8.6	ns	81.4 ± 6.3	81.9 ± 7.1	ns
Lateral	90.2 ± 6.3	95.7 ± 6.8	<0.05	86.7 ± 2.6	94 ± 10.7	ns	88.3 ± 4.8	94.8 ± 8.8	<0.01
Inferior	75.8 ± 5.2	80.8 ± 6.3	<0.01	82.1 ± 8.1	88.3 ± 9.2	<0.05	79.2 ± 7.4	84.8 ± 8.6	<0.001
Septum	75 ± 7	76.2 ± 5.5	ns	75.3 ± 3.1	75 ± 6.7	ns	75.2 ± 5	75.5 ± 5.9	ns

RL = right lateral; ns = not significant.

25. Kobayashi H, Asano R, Oka T, et al. Simultaneous evaluation of myocardial

33. Van Den Berg EK Jr, Popma JJ, Dehmer GJ, et al. Reversible segmental left ventricular dysfunction after coronary angioplasty. *Circulation* 1990;81:1210–1216.

TABLE 3
Semiquantitative Analysis of Supine and RL Imaging in All Myocardial Regions (Segmental Defect Numbers)

Region	Supine (n = 422)	RL (n = 350)	p
Anterior	71 (17%)	74 (21%)	ns
Septum	70 (17%)	68 (19%)	ns
Inferior	130 (31%)	78 (22%)	<00.01
Lateral	97 (23%)	79 (22%)	ns
Apex	54 (13%)	51 (15%)	ns

RL = right lateral; ns = not significant.

rate was applied to patients with a low likelihood of CAD (number of patients with normal images divided by total number of patients with low likelihood of CAD).

RESULTS

The prevalence of CAD was 64% in our study group (Table 1). Men had experienced more previous myocardial infarction (history, electrocardiogram findings and fixed defects on images) and more frequently had a history of smoking as predisposing factors than did women. However, more women were diabetic. The rest of the patient characteristics, including myocardial ischemia by sestamibi studies, were not significantly different.

Regional Myocardial Counts

The ratios of mean counts per pixel in all myocardial regions compared with the apex (the region with the highest counts per pixel) is shown in Table 2. A significant increase in inferior region counts by RL imaging was noticed in both male and female populations when compared with supine imaging. Other regions showed no significant differences, with the exception of lateral region counts, which also was increased to a lesser extent in the RL images, primarily in the male group.

Comparison of Semiquantitative Supine Versus Right Lateral Images

The total number of defects were fewer in the myocardial SPECT RL position images than the supine images (350 versus 422, respectively). When the number of defects was divided by the number of myocardial regions (Table 3), supine inferior defects were 31%, while the same patients with RL inferior defects were 22% ($p < 0.01$). Concerning the severity of the defects in the inferior region, the frequency of mild defects was more in the RL images (46%) than the supine images (31%) ($p < 0.05$), whereas fewer differences were seen in moderate and severe defects (Table 4). Other myocardial regions showed no statistical distinction. In addition, semiquantitative analysis of the segmental defects (means ± s.d.) in all myocardial regions was performed (Table 5). Again, inferior myocardial defects were 1.9 ± 1.2 in supine, which is more abundant than 1.2 ± 1.3 in RL imaging ($p < 0.0001$). Furthermore, the lateral

TABLE 4
Inferior Wall Segmental Defects in Supine and RL Techniques Subclassified by Defect Severity

Technique	Mild defects	p	Moderate defects	p	Severe defects	p	Total
Supine	60 (46%)	<0.05	47 (36%)	ns	23 (18%)	ns	130
RL	24 (31%)	ns	34 (44%)	ns	20 (26%)	ns	78

RL = right lateral; ns = not significant.

TABLE 5
Semiquantitative Analysis of Supine and RL Imaging in All Myocardial Regions (Segmental Defects, Mean ± s.d.)

Region	Supine	RL	p
Anterior	1.1 ± 1.2	1.1 ± 1.2	ns
Septum	1.0 ± 1.5	1.0 ± 1.5	ns
Inferior	1.9 ± 1.2	1.2 ± 1.3	<0.0001
Lateral	1.4 ± 1.9	1.2 ± 1.8	<0.01
Apex	0.8 ± 0.7	0.8 ± 0.8	ns

RL = right lateral; ns = not significant.

myocardial wall showed more defects in the supine than in the RL position; however, this difference was less significant than the difference in inferior defects. A case example is shown in Figure 2, where diaphragmatic attenuation was decreased in RL SPECT images in a 47-yr-old man with atypical chest pain but positive treadmill electrocardiogram. Subsequent coronary arteriography showed no CAD.

Comparison of Sensitivity, Specificity and Accuracy of Imaging

The overall specificity for detecting CAD by RL imaging semiquantitative analysis was 75% compared with 50% by the supine technique, yet sensitivity was similar in the two methods (93%) (Table 6). When considering the RL imaging method, results of individual vessel sensitivity and specificity analysis revealed a substantial improvement in the right coronary artery (RCA) specificity and normalcy rate, with no considerable decrease of the sensitivity. Similar data from other coronary artery vessels showed no remarkable differences when RL and supine SPECT imaging techniques were compared. For example, the case of a 46-yr-old man with angina pectoris and no previous myocardial infarction is shown in Figure 3. RL images showed improvement in his inferior wall defect, whereas the anteroseptal defect remained unchanged from that shown by his supine images. Coronary arteriography done later confirmed a single 85% left anterior descending CAD.

Quantitative Supine Versus RL Comparison

Both the extent of defects (number of pixels) in the RCA territory (11 ± 16 in supine versus 8 ± 14 in RL, $p = 0.001$) and left coronary circumflex territory (12 ± 16 in supine versus 7 ± 12 in RL, $p < 0.0005$) were more significantly deteriorated in the supine than in the RL polar maps. Likewise, the severity of myocardial defects (sum of s.d. below pixel mean) in the distribution of RCA (36 ± 62 in supine versus 27 ± 56 in RL, $p = 0.0001$) and left coronary circumflex (67 ± 90 in supine versus 38 ± 71 in RL, $p < 0.0001$) was more severe in the supine than in the RL images. Other regions in the distribution of the left anterior descending coronary artery showed no notable difference in either defect extent or severity. The overall extent of defects (93 ± 75 in supine versus 76 ± 12 in RL, $p < 0.005$) and severity (431 ± 423 in supine versus 381 ± 464 in RL, $p < 0.05$) were again worse in the supine than in the RL polar maps.

Patient Motion During Imaging

Severe motion was not noticed in either imaging position. Moderate motion was noticed in 2% of both imaging positions. The incidence of slight patient motion during the study was 6% in the RL method, which was less than 15% in the supine one. This difference, however, did not reach statistical significance.

DISCUSSION

Inferior wall artifactual defects in myocardial SPECT images due to diaphragmatic attenuation is a well-known pitfall, which

TABLE 6
Sensitivity and Specificity for Detecting CAD and Normalcy Rate of Patients with Low Likelihood of CAD: Comparison between Supine and RL Imaging Positions

	Sensitivity		Specificity		Normalcy	
	Supine	RL	Supine	RL	Supine	RL
LAD	20/22 (91%)	20/22 (91%)	10/12 (83%)	10/12 (83%)	16/20 (80%)	15/20 (75%)
RCA	18/18 (100%)	17/18 (94%)	7/16 (44%)	12/16 (75%)	11/20 (55%)	18/20 (90%)
LCX	19/23 (83%)	16/23 (70%)	9/11 (82%)	10/11 (91%)	19/20 (95%)	19/20 (95%)
Overall	28/30 (93%)	28/30 (93%)	2/4 (50%)	3/4 (75%)	9/20 (45%)	15/20 (75%)

CAD = coronary artery disease; LAD = left anterior descending; LCX = left circumflex; RCA = right coronary artery; RL = right lateral.

is frequently confronted in daily nuclear medicine studies (*4–10,19*). Despite the optimal energy of the newly introduced ^{99m}Tc-labeled sestamibi, diaphragmatic photon attenuation continues as a cumbersome complication that hinders the diagnostic accuracy of this modality in many patients.

Prone position imaging can overcome the diaphragmatic inferior wall attenuation. Nevertheless, it remains only an alternative method in certain situations, as when inferior wall defects or patient motion creates a particular difficulty in previous supine acquisition. Segall et al. (*12*) studied 34 male patients and 11 normal volunteers (including five females) with SPECT ^{201}Tl studies and demonstrated higher RCA specificity in prone (90%) compared with supine (66%) positions. Images, however, were interpreted qualitatively by one observer. Esquerrè et al. (*11*) also showed a visual and circumferential profile improvement in 17 of 25 retrospective normal ^{201}Tl patients studied (including four females). Kiat et al. (*15*) conducted similar research using ^{201}Tl in 111 male patients. Quantitative assessment of prone position yielded RCA specificity of 94% and sensitivity of 88%. The limitations of this method were increased camera-to-chest wall distance, observation of more anterior/anteroseptal defects and hot spots, less suitability for many women and markedly obese patients and the need for table adjustment with cardiac area cutout. Therefore, the authors recommended the supine position as the imaging position of choice. A similar conclusion was reached by Perault et al. (*13*), using ^{99m}Tc-sestamibi instead of ^{201}Tl. The

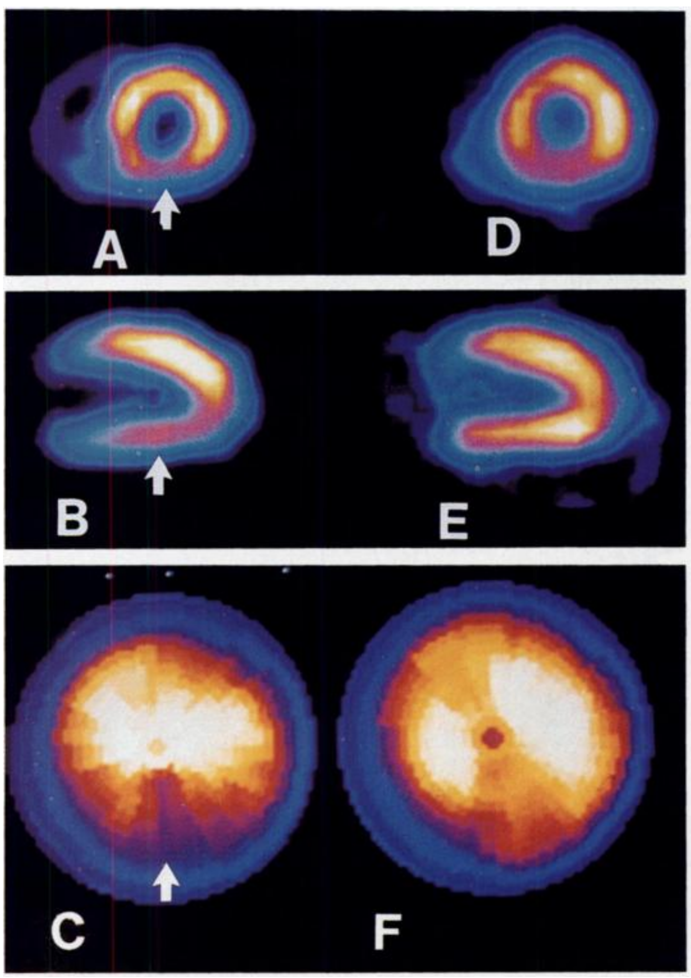

FIGURE 2. SPECT study of a normal patient. Inferior wall attenuation (arrow) is obvious in the exercise supine short axis (A), the vertical long axis (B) as well as the polar map (C). Attenuation is not seen in equivalent RL images (D–F).

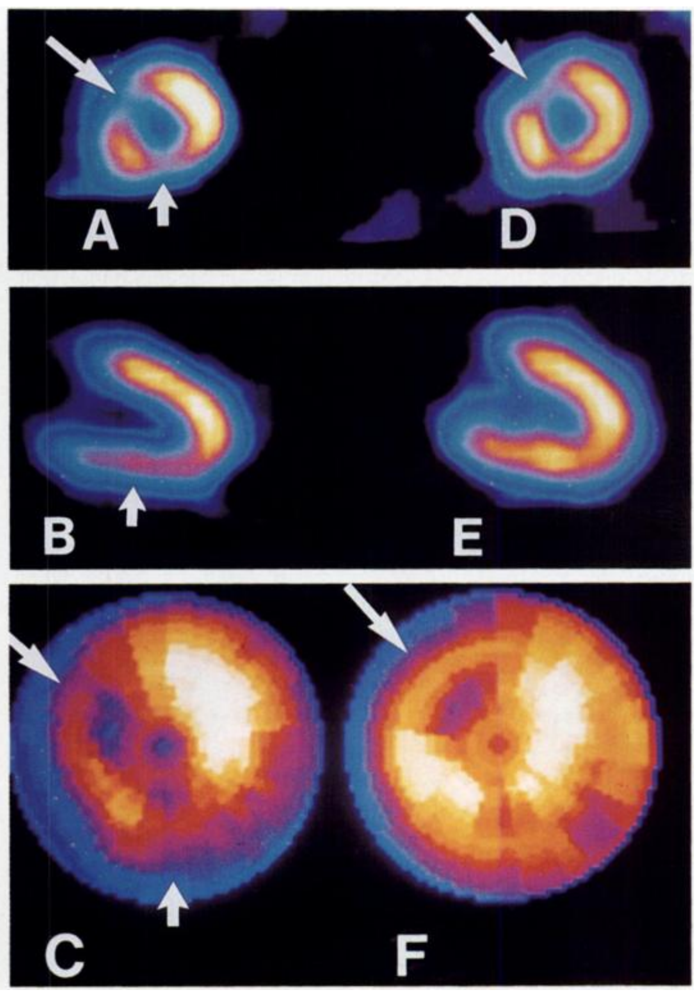

FIGURE 3. SPECT study of a patient with left anterior descending CAD. Supine stress images demonstrate both inferior (small arrow) and anteroseptal (large arrow) defects in the short axis (A), vertical long axis (B) and polar map (C). The same RL images (D–F) reveal improvement of the inferior defect, while the anteroseptal defect remains the same.

quantitative comparison of their 99 male patients revealed improvement of the inferior wall counts, but anterior and lateral wall information was impaired. Recently, O'Conner et al. (*20*), in a phantom study, reported that the average imaging table attenuates 5%–10% of ^{99m}Tc and 8%–12% of ^{201}Tl.

All studies were analyzed quantitatively and semiquantitatively by three expert observers because we were concerned about the objectivity of image examination. Consequently, a rather lower specificity for diagnosing CAD and in particular RCA disease than the usual qualitative assessment was noticed. Our results clearly indicate that, in the same patient, the size and severity of inferior wall defects improve substantially by RL imaging using both types of analyses. These findings, along with the increase of inferior wall counts that our data confirm, highly delineate the degree of diaphragmatic and subdiaphragmatic tissue attenuation seen in the usual supine position, which is diminished by RL imaging technique (Fig. 2). In addition, no obvious artifacts or new clear defects were seen in the RL images when the supine images of the same patient were examined, although a subtle decrease in the anterior wall counts was occasionally noted in the quantitative images. Hence, the diagnostic accuracy of RCA disease and the overall diagnostic accuracy were promoted when correlated with coronary arteriography. In our experience, severe inferior wall defects have never been an obstacle in confirming RCA disease. Milder defects, however, which can be a source of uncertainty in interpretation, are greatly reduced by this new imaging method (Fig. 3). The lateral wall defects also appear to be fewer in number in the RL imaging, principally in quantitative analysis.

Unlike in some previous reports, we were able to compare both supine and RL SPECT imaging directly, since all patients underwent both methods successively. The order of imaging positions after exercise was not of any concern, since ^{99m}Tc-sestamibi does not show significant redistribution within the first few hours as does ^{201}Tl chloride. Therefore, confusion in analysis due to change in radioisotope myocardial distribution in our patients population, between the supine and RL imaging, was not at all expected.

None of our patients reported any particular discomfort during the RL positioning when queried after the completion of the study. Also, no significant difference in the degree of patient motion was noted in any of our patients when both supine and RL SPECT images were compared. In fact, incidence of motion was less in the RL position than the routine supine position. This is presumably due to better fitting of the chest side than the broader back of the chest to the narrow imaging table. Furthermore, the relative absence of major body curvature when patients are on their sides could be another factor that makes this position more comfortable.

CONCLUSION

Myocardial SPECT imaging using RL positioning markedly improves inferior wall attenuation, leading to a substantial increase in CAD diagnostic accuracy. Moreover, this new imaging position is simple, easy to perform, requires no modification in the imaging table or the gamma camera and is tolerable by both women and men.

ACKNOWLEDGMENT

This work was supported by the Kuwait Heart Foundation.

REFERENCES

1. Kiat H, Berman DS, Maddahi J. Comparison of planar and tomographic exercise thallium-201 imaging methods for the evaluation of coronary artery disease. *J Nucl Med* 1989;30:613–616.
2. Kiat H, Maddahi J, Roy L, et al. Comparison of technetium-99m methoxy isobutyl isonitrile and thallium-201 for evaluation of coronary artery disease by planar and tomographic methods. *Am Heart J* 1989;117:1–11.
3. Strauss H, Boucher C. Myocardial perfusion studies: lessons from a decade of clinical use. *Radiology* 1986;160:577–584.
4. DePuey E, Garcia E. Optimal specificity of thallium-201 SPECT through recognition of imaging artifacts. *J Nucl Med* 1989;30:441–449.
5. DePuey G III. How to detect and avoid myocardial perfusion SPECT artifacts. *J Nucl Med* 1994;35:699–702.
6. DePasquale E, Nody A, DePuey E, et al. Quantitative rotational thallium-201 tomography for identifying and localizing coronary artery disease. *Circulation* 1988;77:316–327.
7. Tamaki N, Yonekura Y, Mukai T, et al. Stress thallium-201 emission computed tomography: quantitative versus qualitative analysis for evaluation of coronary artery disease. *J Am Coll Cardiol* 1984;4:1213–1221.
8. Garcia E, Van Train K, Maddahi J, et al. Quantification of rotational thallium-201 myocardial tomography. *J Nucl Med* 1985;26:17–26.
9. Iino T, Toyosaki N, Katsuki T, et al. Evaluation of diseased coronary arterial branches by polar representations of thallium-201 rotational myocardial imaging. *Clin Nucl Med* 1987;12:688–693.
10. Geckle W, Frank T, Links J, Becker L. Correlation for patient and organ movement in SPECT: application to exercise thallium-201 cardiac imaging. *J Nucl Med* 1988;29: 441–450.
11. Esquerrè J, Coca F, Martinez S, Guiraud R. Prone decubitus: a solution to inferior wall attenuation in thallium-201 myocardial tomography. *J Nucl Med* 1989;30:398–401.
12. Segall G, Davis M. Prone versus supine thallium myocardial SPECT: a method to decrease artifactual inferior wall defects. *J Nucl Med* 1989;30:548–555.
13. Perault C, Loboguerrero A, Liehn J, et al. Quantitative comparison of prone and supine myocardial SPECT MIBI images. *Clin Nucl Med* 1995;20:678–684.
14. Lisbona R, Dinh L, Derbekyan V, Novales-Diaz J. Supine and prone SPECT ^{99m}Tc-MIBI myocardial perfusion imaging for dipyridamole studies. *Clin Nucl Med* 1995; 20:674–677.
15. Kiat H, Van Train K, Friedman J, et al. Quantitative stress-redistribution thallium-201 SPECT using prone imaging: methodologic development and validation. *J Nucl Med* 1992;33:1509–1515.
16. Suzuki A, Muto S, Oshima M, et al. A new scanning method for thallium-201 myocardial SPECT: semidecubital method. *Clin Nucl Med* 1989;14:736–741.
17. Yamamoto S, Kitano T, Kanda H, Kondo T, Suzuki A. A comparative study between a new 50-degree right semidecubital scanning and usual supine scanning of thallium-201 myocardial tomography for evaluation of coronary artery disease. *Jpn Circ J* 1991;55:356–364.
18. Garcia E, Cooke C, Van Train K, et al. Technical aspects of myocardial SPECT imaging with technetium-99m-sestamibi. *Am J Cardiol* 1990;66:23E–31E.
19. Kirsch C, Doliwa R, Buell U, Roedler D. Detection of severe coronary heart disease with thallium-201: comparison of resting single photon emission tomography with invasive arteriography. *J Nucl Med* 1983;24:761–767.
20. O'Connor M, Bothun E. Effect of tomographic table attenuation on prone and supine cardiac imaging. *J Nucl Med* 1995;36:1102–1106.